EUROPEAN FUSION DEVELOPMENT AGREEMENT

EFDA–JET–PR(02)09

N.N.Gorelenkov, A.Gondhalekar, A.A.Korotkov, S.E.Sharapov and D.Testa

Mechanisms of Radial Redistribution of Energetic Trapped Ions due to m=2/n=1 Kink Instability in Plasmas with an Internal Transport Barrier in the Joint European Torus

Mechanisms of Radial Redistribution of Energetic Trapped Ions due to m=2/n=1 Kink Instability in Plasmas with an Internal Transport Barrier in the Joint European Torus

N.N.Gorelenkov, A.Gondhalekar[1], A.A.Korotkov[1], S.E.Sharapov[1], D.Testa[2]
and contributors to the EFDA-JET workprogramme*

Princeton Plasma Physics Laboratory, Princeton University, Princeton, NJ 08543, USA
[1]UKAEA/Euratom Fusion Association, Culham Science Centre, Abingdon, OX14 3DB, UK
[2]Plasma Science and Fusion Center, MIT, Cambridge, MA 02139, USA
** See annex of J. Pamela et al, "Overview of Recent JET Results and Future Perspectives", Fusion Energy 2000 (Proc. 18th Int. Conf. Sorrento, 2000), IAEA, Vienna (2001).*

Preprint of Paper to be submitted for publication in
Physics of Plasma

ABSTRACT

Internal radial redistribution of MeV energy ICRF driven hydrogen minority ions was inferred from neutral particle analyzer measurements during large amplitude MHD activity in plasmas with an internal transport barrier in the Joint European Torus. A theory is developed for energetic ion redistribution during a m = 2/n = 1 kink mode instability. Plasma motion during the instability or during subsequent magnetic reconnection generates an electric field which can change the energy and radial position of the energetic ions. The magnitude of ion energy change depends on the value of the safety factor at the plasma core from which the energetic ions are redistributed. A relation is found for the corresponding change in canonical momentum P_φ ,which leads to radial displacement of the ions. The model yields distinctive new features of energetic ion redistribution under such conditions. Predicted characteristics of ion redistribution are compared with the measurements, and good correlation is found. Sometimes the energetic ions were further transported to the plasma edge due to interaction with a long-lived magnetic fluctuation (often in the form of a magnetic island) with chirping frequency in the laboratory frame which developed after the m= 2 /n = 1 kink instability. Convection of resonant ions trapped in a radially moving phase-space island is modeled to understand the physics of such events.

1. INTRODUCTION

Confinement of MeV energy ions, produced either by nuclear fusion reactions or radio frequency heating, in the plasma core is a requirement for succesful heating of tokamak plasmas. Measurement, modeling and bench-marking of internal radial redistribution and expulsion of energetic ions due to tokamak plasma instabilities is therefore a priority topic. Interactions of energetic ions with m = 1/n = 1 kink modes and sawtooth instabilities in plasmas with a core safety factor $q(0) < 1$, and the concomitant redistribution of ions have been extensively studied both experimentally[1, 2] and theoretically[3,4,5]. The search for methods to attain high pressure stable plasmas with strong bootstrap current is at present focussed in the Joint European Torus (JET) on regimes with an Internal Transport Barrier (ITB) with $q(0) > 1$. In the present work we report measurements and modeling of radial redistribution of energetic trapped ICRF heated ions due to the MHD kink instability at the q = 2 surface in ITB plasmas in JET.

High performance plasmas are obtained in several Tokamaks including JET, Tokamak Fusion Test Reactor (TFTR), DIII-D and JT-60U due to formation of an ITB [6]. The barrier formation is attributed to the shape of the q-profile, with generally the central q(0) = 1.5 - 2. Additionally reverse-shear giving a minimum in q(r) at $0.3 \leq r/a \leq 0.5$ seems to reduce the power threshold for entering the ITB regime. In such conditions, where m = 1/n = 1 sawtooth oscillations are stable, other types of MHD modes arise to limit plasma performance. The most common of these are the pressure driven infernal kink modes coupled to the plasma edge [7, 8]. Experiments show that in JET plasmas such dominantly m = 2/n =1 mode activity often reaches very high amplitude, followed by rapid motion of the plasma, invasion of cold plasma into hotter plasma about the q = 2 location, inversion of the

electron temperature profile about the q = 2location, suprathermal electron cyclotron emission, and abrupt change in internal inductance l_i indicating internal magnetic reconnection. In the following we shall refer to such an event as a 'crash'. Experimental evidence for the above-mentioned crash will be presented in section 2 in the discussion of Fig.4 and Fig.5. The crash leads to an internal redistribution of energetic trapped ions. Sometimes the crash is followed by a full disruption of the plasma.

Measurements of confined ICRF heated energetic hydrogen minority ions in ITB plasmas were made using a high energy Neutral Particle Analyzer (NPA) [9]. Using the NPA measurement of the atomic efflux, the line-of-sight integrated energy distribution function, $F(\varepsilon,t)$, of trapped ions at the bounce points of their banana orbit was inferred. Deduction of $F(\varepsilon,t)$ invokes impurity induced neutralization of MeV energy ions, which was discovered in JET [10]. The method has become quantitively well established [11, 12], and has subsequently been widely applied also in JT-60U [13] and TFTR [1]. During hydrogen minority ICRF heating of deuterium plasmas in ITB configurations in JET, often a short sharp burst of anomalously high efflux of MeV energy hydrogen atoms was measured by the NPA. The flux-spike always coincided with n = 1 mode activity culminating in a crash. During the crash the flux to the NPA increased in less than 1ms, which was the minimum time resolution used in the NPA measurements. The subsequent evolution of the flux-spike depended on the magnetic activity following the crash. Sometimes the crash was followed by a long-lived n = 1 magnetic activity with rapidly decreasing frequency ('chirping'). The decay time of the NPA flux-spike during the chirping depended on the energy of the ions measured. Analysis of the measurements leads to the inference that the NPA flux-spike arises due to the ions suffering radial displacement from the plasma core at $r/a \leq 0{:}3$ to locations of much greater neutralization at larger r/a, where they become neutralized, generating the large flux-spike.

The flux-spike measurements were grouped according to whether or not a chirping activity developed. The measurements also yielded a correlation between the magnitude of the NPA flux-spike and the value of the safety factor in the plasma core, q(0), just before the crash. Note that sometimes the NPA flux-spike was also observed when the n = 1mode grew to such large amplitude that the plasma subsequently disrupted. We conjecture that under such conditions magnetic islands may be formed on different resonant surfaces overlap, creating conditions for diffusion in stochastic fields. Then the correlation mentioned above between the measured NPA flux-spike and q(0) was not observed. However, this paper excludes consideration of such disruptive events.

In TFTR [1,3], it was shown that in a m = 1/n = 1 sawtooth crash lower energy trapped ions experienced stronger mixing than the higher energy ones. The observations were in line with theory [3, 4], which predicted such behavior due to faster toroidal precession of more energetic trapped ions then the characteristic crash time τ_{cr} . Faster precessing ions, with $\tau_{pr} << \tau_{cr}$, average out the effect of the m = 1/n = 1helical perturbation and therefore experience less redistribution then the slowly precessing ions, i.e. ions with smaller energy. An expression was derived for the critical energy which separates these two groups of ions

$$\varepsilon_{cr} = \frac{2\omega_c maR}{n\tau_{cr}q} \tag{1}$$

Here ω_c is the ion cyclotron frequency, m is the mass of the energetic ion, a and R are the minor and major radii of the plasma, n is the toroidal mode number, τ_{cr} is the sawtooth crash time or characteristic reconnection time, and q is the safety factor. ε_{cr} is the ion energy at which ion toroidal precession time becomes approximately equal to the sawtooth crash time.

The analysis of NPA measurements of fusion α-particle redistribution due to sawteeth in TFTR [3] was not able to identify within the error bars the way in which ions were redistributed in P_φ during the crash. This was because the NPA line-of-sight was in the equatorial plane perpendicular to the magnetic axis, and therefore only horizontal redistribution of ions could be measured, with the change in ion energy being responsible for it. In ref. [3] two redistribution formulae for crash induced change ΔP_φ were tested, a stochastic distribution given by a large diffusion coefficient, and a distribution derived from Kadomtsev's inversion formula whichinvokes conservation of magnetic flux and number of ions. Using the stochastic model for ΔP_φ gave a uniform ion density distribution in the vertical (Z) direction, whereas using Kadomtsev inversion gave a hollow profile along the Z-coordinate. Both models for ΔP_φ gave satisfactory agreement with the TFTR measurements. The same measurements were also modeled by invoking magnetic field stochasticity due to overlapping multiple poloidal harmonics [5], again giving satisfactory agreement with measurement.

Note that physically application of the inversion formula to trapped ions is based on the presence of an electric field generated by plasma motion during the magnetic reconnection. This means that other types of MHD instability, characterized by rapid plasma motion, such as the kink mode instability, may have similar effects on energetic trapped ions. In the present work we perform a complementary analysis of ion redistribution induced by the crash event in JET ITB plasmas, the crash driven by an m = 2/n = 1 kink instability which does not always culminate in a magnetic reconnection. When it does a long lived magnetic island is formed after the instability developes. Such kink instabilities occur at different values of q(0). This makes it possible to measure ion redistribution as function of q(0) and thereby exclude specific assumptions of modeling used in [3, 5]. We show that the modeling of the JET measurements favours a post-crash distribution of ΔP_φ similar to the sawtooth driven redistribution subject to the Kadomtsev inversion formula. Physically this corresponds to the component of the E xB drift along the direction of minor radius being responsible for the ion redistribution.

In this paper we develop a theory of ion redistribution due to a m = 2/n = 1 kink mode instability. The formalism is applicable to plasmas in which the core safety factor is $1 \le q(0) \le 2$, as in the ITB plasmas considered here. We show that for energetic ion redistribution due to such a crash, theory predicts a strong correlation between spatial range of ion redistribution and q(0). It is also shown that in transport due to subsequent trapping in the chirping n = 1 magnetic fluctuations, ions in a wide energy range can be transported to the stochastic ripple diffusion domain at the plasma edge at the top of the torus.

2. MEASURED ION REDISTRIBUTION AND MHD ACTIVITY

2.1 NPA Measurements show Radial Ion Redistribution

High energy NPA measurements have been used in JET for determining the energy distribution function, $\overline{F}(\varepsilon;\mu^*;t)$, of MeV energy ICRF driven hydrogen isotope [11, 12, 14, 15] and He^{-3} ions [16] with almost fixed ion pitch angle, given by $\mu^* \equiv \cos^{-1}(\upsilon_{||}/\upsilon) \leq 5 \times 10^{-3}$. Measurements of $F(\varepsilon;\mu^*;t)$ for confined DT fusion alpha-particles [17] and knock-on deuterons produced by close elastic collisions between DT fusion alpha-particles and thermal plasma fuel ions have also been made [17, 18]. These measurements rely on non-perturbing neutralization of energetic ions by one- and two-electron species of the main intrinsic plasma impurities, carbon, beryllium and helium [10, 11]. Through these experiments the physical basis of the measurement and deduction of $\overline{F}(\varepsilon;\mu^*;t)$ has become quantitatively well established. The high energy NPA has thus become a key tool for studying the dynamics of confined MeV energy hydrogen and helium isotope ions. Redistribution of ICRF driven energetic hydrogen ions from the plasma core in JET ITB plasmas was deduced from measurements using the methods decribed above. A preliminary account of the measurements has been given earlier [19].

A description of the measurement set-up is given in ref.[11]. The vertical line-of-sight of the NPA crosses the plasma centre at R = 3:1m, and is typically inside the on-axis ICRF resonance. The NPA admits only atoms born on the vertical NPA line-of-sight and from ions with $\upsilon_z/\upsilon_{||} \geq 2 \times 10^2$, where υ_z is the component of ion velocity in the Z-direction. The measured quantity, the flux of energetic atoms to the NPA, is thus

$$\overline{F}(\mathcal{E},t) = \int F(\mathcal{E}, Z, \mu^*, t)\, P(\mathcal{E},Z,t)\, \gamma(\mathcal{E},Z,t)\, dZ \qquad (2)$$

Here, ε is the energy of the ions moving towards the NPA, Z is the vertical coordinate, $F(\mathcal{E}, Z, \mu^*, t)$ is the local energy distribution function of ICRF driven ions with ε typically extending to many MeV, $P(\mathcal{E},Z,t)$ is the local neutraliza-tion probability for the energetic ions, and $\gamma(\varepsilon,Z,t)$ is the plasma transparancy for the exiting energetic atoms. The integral is along the NPA line-of-sight. In ICRF heated plasmas in JET with the resonance located on the plasma axis, the radial ICRF heating profile is approximately Gaussian of width 0:2 – 0:3m [12]. Thus in eq.(2) $F(\mathcal{E}, Z, \mu^*, t)$ is weighted to the plasma core with the dominant contribution coming from r=a < 0:3. $P(\mathcal{E},Z,t)$ is the sum of contributions from different hydrogen isotope atoms (thermal and NBI) in the plasma and from the one- and two-electron ions of the main intrinsic plasma impurities, carbon, beryl-lium and helium. In JET the dominant neutralization agents for high energy hydro-gen isotope ions are [H]- and [He]-like impurity ions. The density of these ions, produced by charge-exchange reactions, is sustained by the density of hydrogen isotope atoms and that of the bare impurity ions [10, 11]. The source for both the hydrogen atoms and the impurities is at the plasma edge. In JET plasmas gener-ally $P(\mathcal{E},Z,t)$ is nearly constant in the plasma core and increases rapidly in the region 0:6 ·≤| $Z=b$ |≥j· 1. In ICRF heating experiments, using measurements of $\overline{F}(\mathcal{E},t)$ and knowing $P(\mathcal{E},Z,t)$ and $\gamma(\mathcal{E},Z,t)$ from measured plasma parameters,

the line-of-sight integrated ion energy distribution function $\overline{F}(\mathcal{E}, Z, \mu^*, t)$ is routinely deduced.

Fig.1 shows evolution of a deuterium ITB plasma pulse in JET, heated with deuterium NBI and first harmonic hydrogen minority ICRF heating, which produces the MeV energy hydrogen and deuterium ions with $T_\perp \leq T_\parallel$ and effective tail temperature of $0.2 \leq T_\perp$ (MeV) ≤ 0.4. The eight measurement channels of the NPA detected hydrogen atoms spanning the range $0.3 \leq \mathcal{E}_H$(MeV) $\leq$ 1.1.The key observation was that at 4.725s a sharp increase, by a factor of $3 - 5$, in the flux to the NPA was measured in the whole measurement energy range. Simultane-ously a sharp increase in n = 1 mode activity was measured on the external Mirnov coils, immediately followed by an ELM seen on the D_α signal. This pattern was common to all of the large number of pulses in which energetic ion redistribution was inferred. The NPA flux-spike was observed in the hydrogen as well as in the deuterium flux. Often such events caused loss of ICRF power coupling as seen in Fig.1, thought to be due to the ELM. The burst of n = 1destroyed the internal transport barrier, evidenced by degradation of thermal diffusivity, fusion reactivity, and plasma rotation shown in Fig.1. For completeness, just before the n = 1 burst the peak electron density ne(0) ~ 3.5×10^{19} m^{-3}. Note that the duration of the NPA flux-spike, the n = 1mode activity, the ELM seen in D_α emission, and the subsequent redistribution of ions to be discussed, were much shorter than the slowing-down time of the ICRH driven ions in the measurement energy range. We therefore assume that for modeling the subsequent short duration energetic ion transport, the loss of ICRH coupling, if it occured, may be neglected. In nearly half the pulses in a large set of pulses where the flux-spike was observed, a loss of ICRH coupling or a full disruption of the plasma was observed subsequent to the NPA flux-spike. However, fast 48-channel internal ECE emissivity measurements of T_e (r) showed a sawtooth-like crash with inversion radius of R ≈ 3.6m. EFIT equilibrium reconstruction, using only external magnetic measurements, showed that just before the n = 1burst q = 2was located at major radius R ≈ 3.54m. ECE measurements also showed formation of an island, similar to an island after a sawtooth crash, at R ≈ 3.6m.

We exclude transient increase in neutralization probability in eq.(2), due to ELM related injection of H/D atoms or impurities into the plasma, as cause of the NPA flux-spike. This is because: (1) the ELM occured later than the NPA flux-spike, (2) the ELM related increase in impurity density in the plasma decayed on a time scale much longer than the flux-spike duration, (3) disturbance of impurity ionization balance in the plasma due to injection of H/D atoms from the plasma edge must relax throughout the plasma after the ELM(600μs wide) in ≤ 400μs, contrary to the measured $5 - 10$msec width of the flux-spike, (4) if ELM induced increase in neutralization probability were the cause of the flux-spike then the de-cay time of the flux-spike in the low energy NPA channels would be shorter than or equal to that in the high energy channels. The measured decay time of the flux-spike is longer for the low energies than for high energies, varying over $4 \rightarrow 2$ms for energies E (MeV) = $0.3 \rightarrow 1.1$. For reasons (1)-(4) we conclude that the measured time evolution of the flux-spike is contrary to expected evolution if ELM related transient enhancement of neutralization probability had taken place. We therefore exclude the ELM as cause of the NPA flux-spike. This conclusion is

validated by the observation that in many similar ITB plasma pulses ELMs occured without a corresponding NPA flux-spike.

First evidence that the flux-spike corresponded to expulsion of ICRF driven ions from the plasma core was seen in the spectrogram of B_θ fluctuations measured at the plasma edge using Mirnov coils. Typically high frequency EAE(350-400 kHZ) and TAE(100-180 kHZ) modes, excited by energetic ICRF driven ions, were abruptly extinguished at the time of the flux-spike, analogous to termination of TAE activity by giant sawteeth in TFTR [20].

Fig.2 shows the temporal behaviour of the NPA flux-spike in a pulse where the n = 1 burst was followed by chirping long-lived magnetic fluctuations. Energy dependence of the decay times shown is typical. It looks similar to that for sawtooth induced redistribution observed in TFTR [1], where the ions first suffer fast expulsion from the plasma core and subsequent slow loss due to stochastic ripple diffusion. The measured decay time of the flux-spike was modeled using the ORBIT guiding centre code [21] and was consistent with the fact that the highenergy ions generally diffused faster from the con£nement region due to the energy dependence of the magnetic field ripple stochastic diffusion.

We have applied ORBIT to JET ITB plasmas, incorporating JET TF-ripple and the measured pre crash plasma equilibrium. Since stochastic ripple diffusion is very sensitive to the magnitude of the TF ripple and the ion energy, we can deter-mine the allowed position of the ion bounce point r_{bp} at which it was neutralized. For example, for low energy ions with $\mathcal{E} \simeq$ 300keV we obtain the post-crash mi-nor radius of the bounce point at $r_{bp} = a \simeq 0.75$, while for higher energy ions with $\mathcal{E}$ = 800keV we find $r_{bp} = a \simeq 0.67$. Without the stochastic ripple diffusion the ions would live at given minor radius for a long time, comparable to the slowing-down time of several hundred milliseconds. Note that in JET, because of the small amplitude of the TF ripple due to its high periodicity (32 TF coils), the spatial extent of the stochastic ripple diffusion domain is small and typically is around $\Delta r = a \simeq 0{:}05$ between the con£nement domain and the prompt loss domain. Since (1) the width of the ripple diffusion region is so narrow, (2) the flux-spike time coinsides with the chirping frequency magnetic activity and (3) ceased after it, we can conclude that the time dependence of the NPA flux after the crash is primar-ily controlled by the chirping frequency magnetic activity and is coming from this narrow region of the stochastic ripple diffusion. Using the ORBIT modeling we determine that the bounce points of ions giving the flux evolution shown in Fig.2 have to be located within $1.39 \leq Z(m) \leq 1.55$.

With this information in hand we were able to determine the energy distribution function of ions contributing to the flux-spike. Before and after the flux-spike the position of ions was at $r/a \leq 0.3$, permitting an accurate determination of $\overline{F}(\mathcal{E}; t)$. Fig.3 shows the deduced absolute energy distribution function of the ions at two times, just before and after the flux-spike. The relative energy distribution functionof ions contributing to the flux-spike is also shown. Due to uncertainty in impurity transport in the edge plasma from which the flux-spike originates, the required impurity ionization equilibrium can not be computed accurately [11]. Therefore the absolute magnitude of the ion energy distribution function in the flux-spike can not be determined accurately, although variation with energy is correctly

deduced. Therefore in Fig.3 the energy distribution function of ions contributing to the flux-spike was normalized to that before and after the flux-spike at the highest energies. From Fig.3 we conclude that more low energy ions with E · 0:6MeV are redis-tributed than higher energy ones. Comparison of deduced ion energy distribution functions before and after the NPA flux-spike, in the range $0.3 \leq \mathcal{E}$ (MeV) ≤ 1:1, shows that 10 ÷ 20% of the ICRF heated ions in the measurement phase-space were redistributed from the plasma core due to the crash, and that the affected ions were those with toroidal precession time greater than the crash time, $\tau_{pr} > \tau_{cr}$.

2.2 m = 2/n = 1 Instability and Subsequent Long-lived Magnetic Fluctuation with Chirping Frequency

Formation of an ITB in JET plasmas leads to a high gradient in the pressure profile, close to the limit of stability of pressure driven kink modes. According to ref.[7] disruptions are the most common limit to ITB plasmas in JET. The measured structure of the disruption precursor mode was found to be in agreement with calculated structure of the ideal MHD n = 1pressure driven kink mode. Analysis in ref.[7] suggests that when conditions are unfavourable the precursor mode grows to large amplitude simultaneously with plasma rotation decreasing, so that eventually the mode locks and a disruption occurs. Sometimes the mode does not grow to such large amplitude as to cause mode locking or disruption, but the ITB is destroyed nevertheless.

Ref.[7] also shows that fishbone-like activity frequently occurs in JET ITB plasmas. Frequency chirping is a notable characteristic of the modes, with frequency (f) down-shifting at a rate df/dt ≈ -3×10^{6} Hz/s, with duration 5 – 10msec. One possible mechanism for these oscillations is the m = 2/n = 1 kink mode in plasmas with off-axis minimum in q(r), driven unstable by precessional resonance with energetic ions [22]. Degradation of ITB and plasma performance can be as-sociated with such fishbone-like activity. Separate NPA measurements during such fishbone-like activity show no detectable change in NPA flux. This leads to the inference that any concommitant internal redistribution of energetic ions, if at all, must be small in spatial extent. The resistive reconnecting counterpart of the above, a double-tearing mode leading to sawtooth-like reconnection at the q=2 surface was observed and analyzed in TFTR [23].

The most prominant magnetic activity present at the time of the NPA flux-spike is shown in Fig.4, where the dominant behaviour is the fast magnetic instability with possibly a magnetic reconnection soon after 4.724s. Evidence of reconnection was not always found in the measured plasma parameters in the pulses studied. In some cases the internal inductance li showed a jump at the time of the crash. For Pulse No: 45837, there was no jump in measured li at the crash, but ECE emissivity measurements showed a sawtooth-like electron temperature inversion radius at R ≈ 3.6m. For comparison we analysed behaviour of measured l_i in pulses with the m = 1/n = 1sawtooth instability. Although l_i jumped at some sawteeth, it did not do so for all sawteeth. Moreover, for the pulses studied, the time resolution of l_i determination was very long (20-70ms) compared to any reconnection time-scale. We conjecture that in both cases, of m = 1/n = 1and m = 2/n = 1crashes, absence of change in l_i probably indicates incomplete reconnection, or simply defficiency in the l_i measurement.

Comparing T_e (r) before and after the instability we see that T_e (r) increases outside the q = 2surface as shown in Fig.5, indicating plasma mixing. Cross-correlation analysis of magnetic fluctuations and 48-channel internal ECE measurements of T_e (r), during the long-lived mode phase, suggest that the magnetic perturbation formed has large radial width of up to 30cm, with an island of width ≈3cm formed near the q = 2 surface. At the q = 2 surface the phase of the electron temperature perturbation changes sign.

The considered instability terminates the ITB, analogously to that described in ref.[7]. The precursor is an n = 1mode of amplitude $\delta B_\theta = B \simeq 2 \times 10^{-4}$, growing up to $\delta B_\theta = B \simeq 2 \times 10^{-3}$ during the crash. In some pulses a long-lived magnetic fluctuation in the form of magnetic island was created, such as the one shown in Fig.4 with frequency chirping in the laboratory frame from 15kHz to 4kHz within ≃ 6ms, giving df/dt $\simeq -2 \times 10^6$ Hz/s. Fig.4 shows the crash at t = 4.7245s while Fig.5 shows it at t = 4.7266s, the timing discrapancy of ≈2:1ms is due to averaging and Fourier transformation required in computing the magnetic spectrogram. At the q = 2 location, the measured rate of change of plasma rotation frequency was $df_{rot} / dt \sim -7{:}5 \times 10^4$ Hz/s. Thus deceleration of the magnetic island in the plasma frame is the main cause of the observed frequency chirping.

3. FORMULATION OF ENERGETIC ION REDISTRIBUTION DURING A m=2/n=1 INSTABILITY

In this section we present a theory of redistribution of energetic ions induced by the first, fast growing part of the crash in JET ITB plasmas, which is associated with plasma motion during the instability. The plasma motion sometimes induced long-lived magnetic activity as seen in Fig.4, corresponding to the island mentioned earlier. This is typically a very fast process, with a period shorter than the toroidal precession time of the MeV energy hydrogen ions, but longer than the character-istic transit and bounce times of such ions. We model the NPA flux-spike mea-surements described above, with the aim to elucidate the physical mechanism of ion redistribution. To this end a mechanism for changing the energy of the ions during the m = 2/n = 1 instability is invoked. This mechanism has been developed previously to model sawtooth induced major radius redistribution of DT fusion α-particles in TFTR [3].

3.1 Initial Spatial Distribution of Ions and Bounce Point Characteristics During the Instability

Following Ref.[3] we make use of invariants of ion motion, which are integrals of the guiding-center drift orbit of the ions in the unperturbed tokamak magnetic field. We define three invariants which will be the variables describing the energetic ion distribution function $f(\mu, P_\varphi, p)$

$$P_\varphi \simeq \bar{\psi} - \nu_{\|} R, \; p = \mu B_0 R_0 / \varepsilon, \; \varepsilon = \nu^2 / 2. \qquad (3)$$

Here P_φ is the canonical toroidal momentum, which is not conserved during the instability. $\bar{\psi} = \omega_{c0}\psi/2\pi B_0$ in which ω_{c0} is the ion cyclotron frequency and B_0 is the equilibrium toroidal magnetic

field at the plasma axis. φ is the poloidal magnetic flux. $\mu = \varepsilon_\perp / B$, the ion magnetic moment in which $\varepsilon_\perp$ is the perpendicular ion energy, is assumed to be conserved in the low frequency mode oscillations under consideration. The total ion energy ε or equivalently p, a pitch-angle like variable whose magnitude is equal to the major radius of the bounce point of the ion orbit in a low-beta plasma, are not conserved. The effect of the kink instability on the ions is governed by the ion motion in the presence of an electric field. We assume that the observed instability is driven by the ideal n = 1kink mode which has helical symmetry. To determine the position of the ions after the instability we calculate evolution of ion energy ε and toroidal momentum P_φ through the instability using the following equations

$$\begin{array}{rcccl} \dfrac{dP_\varphi}{dt} & \simeq & \dfrac{d\bar{\psi}}{dt} & = & \langle \nabla\bar{\psi} \cdot v_{E_\perp} \rangle \\ & & \dfrac{d\varepsilon}{dt} & = & z \langle v_{dr} \cdot E_\perp \rangle \end{array}, \tag{4}$$

where z is the ion charge, and v_{dr} is ion drift velocity in the toroidal magnetic field of the tokamak. The equations reflect ion drift in the electric field $E_\perp$ generated by plasma motion during the kink mode instability, and the change of ion energy due to the electric field. The angle brackets denote time average over the ion bounce period. Eq.(4) also describes the evolution of the position of the bounce point, since $d \ln p = -d \ln \varepsilon$: The equilibrium magnetic field can be represented in the form $B = gR\Delta\varphi + \Delta\varphi \times \Delta\psi$, enabling us to transform Eqs.(4) into the set

$$\begin{aligned} \frac{dP_\varphi}{dt} &= -\frac{c\omega_c}{2\pi B^3} \frac{gr}{J} \frac{\partial}{\partial\theta} \phi \\ \frac{d\varepsilon}{dt} &= -\frac{c}{B^2} \varepsilon \left(2 - \frac{pB}{B_0 B_0}\right) \frac{gr}{J} \left[-\left(\frac{\partial}{\partial\theta} \ln B\right) \frac{\partial}{\partial\psi} + \left(\frac{\partial}{\partial\psi} \ln B\right) \frac{\partial}{\partial\psi} \right] \phi \end{aligned} \tag{5}$$

Here J is the Jacobian, and we have used the large aspect ratio approximation $\in^2/q \langle\langle 1$. In general the plasma displacement needs to be found numerically from the Kadomtsev like reconnection model or from MHD for kink instability. Analytic solutions, yielding the main properties of ion motion, are obtainable by making assumptions of ideal MHD electrostatic potential with one dominant mode poloidal harmonic (m; n). Quasineutrality condition can be written as

$$\Delta\phi \simeq \left(\frac{1}{\rho}\frac{d}{d\rho}\,\rho\,\frac{d}{d\rho} - \frac{m^2}{\rho^2}\right)\,\phi = 0,$$

which has a solution near the plasma center $\phi = \phi_0 \rho^m \cos(m_\theta - n\varphi - t)$: The potential takes the familiar form for the m = 2/n = 1 mode inside the mixing radius, as discussed in Ref.[3]. For trapped ions the toroidal angle satisfies $\varphi = \varphi_{md} + q_\theta$, where φ_{md} is the toroidal angle where the ion intersect the midplane. Substituting this formula into Eq.(5) after some algebra keeping finite ellipticity k of

plasma surfaces, we obtain the following equations describing the minor and major radii of the ion bounce points during the crash,

$$\begin{aligned} \frac{d\rho(P_\varphi)}{dt} &= A\rho^{m-1} \sin(n\varphi_{md} + \omega t) \\ \frac{dp}{dt} &= C\rho^{m-1} \sin(n\varphi_{md} + \omega t) \end{aligned}, \tag{6}$$

The coefficients A and C

$$\begin{aligned} A &= \langle -\frac{c}{B}\frac{m}{k}\phi_0 \cos[(m - nq)\theta] \rangle \\ C &= \langle -\frac{c}{B}\frac{m}{k}\phi_0 \cos[(m - nq - 1)\theta] \rangle \end{aligned} \tag{7}$$

The coefficients A and C in Eqs.(6) reveal an important property of ion interaction with the perturbation given (m; n), that the ion mixing will depend on the safety factor. Ion toroidal precession velocity φ_{md} determines the toroidal angle $\varphi_{md} = \dot{\varphi}_{md}t + \varphi_0$, where φ_0 is the pre-crash toroidal angle. Generally Eq.(6) can be solved only numerically, but simple approximations yield all qualitative features of the ion motion. We assume that coefficients A and C remain constant and that the trapping parameter for the ions does not change due to the redistribution, i.e. κ= const. The trapping parameter is given by $\kappa^2 = (1 - \epsilon)[R_0(1 + \epsilon) - p] = 2\epsilon p$, so that for trapped ions κ<1 and for passing ions κ>1. A second approximation that we have made use of is that the period of toroidal precession of the ion is longer than the crash time, $\tau_{pr} > \tau_{cr}$, so that the ion energy is less than the critical energy E cr given in Eq.(1). Recall that low energy trapped ions satisfying $\tau_{cr} < \tau_{pr}$ undergo the largest energy exchange and maximum bounce point displacement. We have varified that in Pulse No: 45837 at t = 4.725sec, at the position of q = 2, for hydrogen ions with $\mathcal{E} \leq 0.4$ MeV, that $\tau_{pr} > \tau_{cr}$(~50μsec). A comparison of correlation between degree of mixing and the ion energy, for different energies, for ion redistribution by sawteeth was made in [1, 3], where it was demonstrated that higher energy ions are less sensitive to the mixing. Then we can write the post-crash minor and major radius positions of the ion bounce points, p_+ and p_+, in terms of the pre-crash values, p_- and p_-,

$$\begin{aligned} \rho_+ &= \rho_- e^{A\tau_{cr}} \sin n\varphi_0 \\ \rho_+ &= \rho_- + \frac{C}{A}(\rho_+ - \rho_-) \end{aligned} \tag{8}$$

From this equation one can determine the ion distribution after the crash if the distribution before the crash is known. We specify the minor radius(ρ) and pitch angle(p) distribution of the ions before the crash as a Gaussian with a peaked spatial profile

$$f_- = (1 - r^2)^4 \exp[-(p - R_c)^2 \Delta_R^{-2}] \tag{9}$$

Here R_c is the position of the ICRF resonance, Δ_R is the radial width of the resonance layer, and R_0 = 3.1m is the major radius of the magnetic axis. Measurements over a wide range of plasma

parameters in TFTR [1] have demonstrated the validity of using such a pitch-angle distribution function for the energetic ions. An important conclusion to be drawn from Eq.(6) is that during mixing following the crash the relation $\dot{p} = C\dot{\rho}/A$ holds. It follows that $\Delta R = \Delta\rho \simeq$ const, where the value of the constant depends mainly on the value of core safety factor q(0).We will consider two limits q(0) = 2 and q(0) = 1, and the perturbation has dominant m = 2harmonic. In the zero orbit width approximation, for q(0) = 1 we obtain

$$\frac{C}{A} = 2\,\frac{E(\kappa)}{K(\kappa)} - 1$$

Here K and E are the complete elliptical integrals of the first and the second kind respectively. Fig.6 illustrates the dependence of the spatial ion redistribution due to the m=2/n=1 instability on the magnitude of the core safety factor q(0). The figure presents contours of the initial ion distribution according to Eq.(9), and trajectories along which the trapped ion bounce points can move as given by Eqs.(8).

From Fig.6 we see that for q(0) = 2a much larger flux to the NPA is to be expected after the crash, because the ion motion is predominantly vertical into the region of rapidly increasing neutralization of the energetic hydrogen ions. In this illustration we have fixed the trapping parameter at κ= 0:6, which corresponds to ions with bounce points just inboard of the major radius. Since the ion mixing due to the crash is not very sensitive to the trapping parameter, for the purpose of a qualitative explanation this is sufficient.

3.2 Mixing Formula

Here we express the energetic hydrogen ion distribution function f_+ after the crash in terms of $f\_$, the distribution function before the crash. Ion redistribution depends on the toroidal angle of the ion position. To obtain the post-crash spatial distribution of the ions integration over pre-crash toroidal position of the ions φ is performed. After the crash the ions will precess toroidally and redistribute homo-geneously over the toroidal angle. We find

$$\begin{aligned} f_+(\rho(\rho\_,R\_),R(\rho\_,R\_)) &= J^{-1}\int f\_(\rho\_,R\_)\,J\_\frac{d\varphi\_}{2\pi} \\ &= J^{-1}\int f\_(\rho',R + C(\rho'-\rho)/A)G(\rho',\rho)J\_d\rho' \end{aligned}$$

We have used Eq.(8), and J is the Jacobian of the transition from the six dimensional phase-space to variables μ, P_φ, p, plus three ignorable fast rotational variables. $G(\rho', \rho)$is defined as

$$G(\rho', \rho) = \frac{1}{2\pi\rho n\sqrt{t_{cr}^2A^2 - [ln(\rho'/\rho)]^2}}. \qquad (10)$$

The amplitude of the electric field potential during the crash has to be determined empirically from plasma measurements. The amplitude will depend on the time duration over which the redistribution

happens, which is usually a few hundred mi-croseconds; and there is large uncertainty in the onset of the event and its duration. For simplicity we fix the potential by specifying τ_{cr} A = 1at the location of the q = 2 surface, thereby picking the strongest redistribution which is equivalent to the reconnection as in the Kadomtsev model. Substituting in Eq.(10) we can now £nd the spatial distribution function of the ions after the crash. This is shown in Fig.7 for two cases, when q(0) = 1 and when q(0) = 2.

In Fig.8 we show the ion distribution after the crash, along the vertical(Z) and horizontal(R) torus coordinates, for q(0) = 1and q(0) = 2. We readily see an important prediction of the foregoing theory, that after the instability the redistri-bution of ion bounce points in the direction of the Z-axis is much stronger when q(0) = 2 than when q(0) = 1. In the latter case ions are redistributed further from the center in the direction of the R-axis.

4. COMPARISON WITH MEASURED ION TRANSPORT

In this section we show that the NPA measurements support the conclusion of the theory above, that the direction of motion of ion bounce points during an m =2/n = 1instability is determined by the magnitude of q(0), and that as the value of q(0) increases from unity, the ion bounce orbit becomes more and more elongated in the direction of the Z-axis.

Continuing from eq.(2) we recall how the NPA flux Γ *(E, t)* is formed. For the pulses under discussion, between r/a = 0 and r/a = 0.8, the measured density of bare carbon ions increased by a factor $\cong$ 2:5, and the modeled density of recycled thermal hydrogen isotope atoms increased by a factor $\cong$ 30. Therefore, bearing in mind the uncertainty introduced due to lack of knowledge of impurity ion transport in calculating the ionization balance, in r/a = 0 $\rightarrow$ 0.8 we expect *P (Z)* to increase substantially, by a factor $\geq$10. Having excluded a transient temporal increase in *P (E, Z, t)*, we infer that the flux-spike must be due to transport of all or some of the energetic ICRF driven ions from the plasma core to outer regions of the plasma in the direction of the NPA. We can now construct Γ_+/Γ_-, the ratio of flux to the NPA at the peak of the flux-spike to that of flux just before the flux-spike, in the lowest energy channel. Formulating the ratio, dropping μ^* and $\varepsilon = \varepsilon^*$ for the lowest energy channel from the notation, we get

$$\frac{\Gamma_+}{\Gamma_-} = \frac{F(Z_+, t_+)\, P(Z_+, t_+)\, \gamma(Z_+, t_+)}{F(Z_-, t_-)\, P(Z_-, t_-)\, \gamma(Z_-, t_-)} \qquad (11)$$

Since the pre-crash location of the energetic ICRF driven ions is in the plasma core, $Z_- \simeq 0$. We now assume that the energetic ion distribution function in the flux-spike is a fixed fraction of the distribution function before the spike, and that the fraction is constant amongst all the pulses in our comparison, thus $F(Z_+, t_+) = F(Z = 0; t_-) = \delta_1 \leq 1$. Similarly, we assume that the transparancy γ from the plasma core at Z = 0 is a fraction of the transparancy from the position Z_+ and that the fraction is constant amongst all the pulses in our comparison, $\gamma(Z = 0, t_-) = \gamma(Z_+; t_+) = \delta_2 \leq 1$. This is reasonable since the plasmas in the comparison have all similar ne and T_e profiles in magnitude and

shape. Then we readily see from eq.(11) that

$$\frac{\Gamma_+}{\Gamma_-} \propto \frac{P(Z_+)}{P(Z=0)} \qquad (12)$$

Since *P (Z)* is a monotonically increasing function of Z, the ratio Γ_+/Γ_- is a measure of how far from the plasma core the energetic ions have been redistributed by the crash, that is to say the $\Gamma_+/\Gamma_- \propto Z_+$. We have evaluated the variation of Γ_+/Γ_- with q(0, t_) for pulses with m = 2/n = 1 kink mode instability. This is shown in Fig.9. Two groups of pulses for which this relationship has been evaluated are shown, one in which the instability occured alone and another in which the crash was followed by a long-lived magnetic fluctuations with chirping frequency. The majority of such magnetic fluctuations can be shown to have a magnetic islands. We deduce from the Fig.9 that (1) for the group with the kink instability alone, that Z_+ increases, or in other words the bounce orbit becomes more and more elongated along the Z-axis, as q(0) increases above unity, (2) with subsequent trapping in a chirping frequency magnetic fluctuations the ions are transported even further along the Z-axis.

5. INSTABILITY INDUCED n = 1 MAGNETIC FLUCTUATION WITH CHIRPING FREQUENCY

In some pulses the instability induces a relatively long-lived (~5 – 8msec) magnetic fluctuation in the form of a chirping magnetic island in which the frequency changes from f = 15 → 4kHz during t = 4:725 → 4:731s, as that shown in Fig.4. We conjecture that such a magnetic island traps and transports energetic ions to the plasma edge where they are lost due to stochastic ripple diffusion or as prompt losses. Ion motion in a decelerating wave has been analyzed previously [24]. It was shown for a tokamak plasma that if the frequency chirping is small then the ion adiabatic invariants are conserved, and if $df/dt < 0$ then the minor radius where the wave-ion resonance occurs, $r_{res}(f)$, will expand. In this section we model how such a mode would, as observed, redistribute ions up to the stochastic ripple diffusion domain at the plasma edge. We assume that the post-crash chirping magnetic fluctuations have the same spatial structure as the pre-crash m = 2/n = 1 infernal kink mode. The most important for the mode-ion interaction is the kink symmetry of the mode and evolution of its rotation frequency, which determine the particle motion near the resonance in phase-space. Since the amplitude of the mode is much smaller than the equilibrium magnetic field, the radial structure of the perturbation and its amplitude account for how strong the interaction is. For use in the next section the kink mode structure was reproduced using an ideal MHD code and plasma rotation was taken from measurements. The spatial structure of the n = 1mode was calculated using the ideal MHD stability code NOVA [25]. Validated plasma parameters, taken from analysis of the pulse using the TRANSP code[26], were employed. We computed the mode structure in Pulse No: 45837 just before the crash using the following parameters: major radius of plasma geometrical center R=2.9m, major radius of plasma magnetic axis R_0=3.1m, plasma minor radius a=0.95m; magnetic £eld at the geometrical center B_φ = 2.56T, central and edge values of the safety

factor q(0)=1:73 and q_a=4:5, respectively. There was no conducting wall around the plasma in this calculation. Fig.10 shows the calculated poloidal harmonics of the component of plasma displacement ξ perpendicular to the equilibrium flux surfaces multiplied by $\nabla\Psi$, where Ψ is the normalized poloidal flux. $\xi \cdot \nabla\Psi$ is plotted as a function of $\sqrt{\Psi}$. First three poloidal harmonics of the unstable n = 1 infernal kink mode are important, of which the m = 2 is dominant. The mode harmonics extend over the whole minor radius of the plasma. The q = 2 surface is located at r/a = 0:6.

5.1 Convective Transport due to Trapping of Ions in Phase-space Island

The ORBIT code [21] was used to simulate the observed energetic ion transport due to the chirping m = 2/n = 1 mode. Calculations indicate that indeed energetic ions with energy E = 200 – 800keV are redistributed in minor radius from the central regions when the amplitude of the perturbed magnetic field is greater then 10^{-3} B_φ. In the following we identify the transport mechanism as convective, and not driven by stochasticity due to overlapping resonant modes. In the convective type of transport ions trapped in a phase-space resonance island near the resonance are transported with the radially moving phase-space resonance island. In our case the resonance island moves as the mode frequency decreases. Since the ion precession frequency is comparable to the toroidal plasma rotation frequency, the plasma rotation needs to be simulated. A radial electric field is therefore included in the calculations. We model it to fit the experimentally measured rotation frequency, giving a best fit electric field potential $\phi = \phi_0 \Psi\ (1 - 0.95\ \Psi^{0.54})$ with the $\phi_0 = -1.2$keV .

An example of ion redistribution is shown in Fig.11 for $\phi_0 = -1.5$keV. The perturbed magnetic field used is of the form [21] $\delta B = \nabla \times \delta\alpha B$. The amplitude of the perturbation, $\delta\alpha_0 = 2 \times 10^{-3} \simeq \delta B/B$, is a normalization constant. In this study we only want to demonstrate the mechanism of transport, so for simplicity we have taken for the initial energetic ion density a flat spatial distribution extending to r/a $\simeq$0:7, as shown in Fig.11(a). A total of 2000 ions were used in the calculations. In Fig.11(b) we see that after the chirping activity the resonant ions are redistributed outward in minor radius (ρ), while some of them are lost.

To understand the nature of this redistribution we plot in Fig.12 the toroidal precession frequency of a 200keV hydrogen ion as a function of normalized poloidal flux taken at the bounce point of the ion drift orbit. Two cases are shown, one with $\phi_0 = 0$, thus with zero radial electric field. In the second case $\phi_0 = -1.2$keV giving a finite electric field. The initial frequency of the kink mode perturbation is f = 15kHz or $\omega = 0.94 \times 10^5$ $\sec^{-1}$. From the figure one can see that the electric field correction to the ion precession frequency moves the resonance from near the plasma core to middle of minor radius and further out as the frequency chirps down further.

Figure 13 presents more evidence that the electric field is critical in describing the convective wave-ion resonance. Figure 13(a) shows dependence of $< \Psi^2_{\text{bounce}} >$, squared poloidal flux at the ion bounce point averaged over the ion distribution, as function of electric field potential ϕ_0 and $\delta\alpha$. Also shown are the same dependencies for the ion loss N_{loss}. As pointed out earlier, with stronger electric field the resonance moves outward so that the increase in averaged ion minor radius or

$< \Psi^2_{bounce} >$ with growing electric field is expected. On the other hand there is only weak dependence of this parameter on the mode amplitude. It would be strong function of the mode amplitude if the stochastic transport is present [27]. Ion loss increases as the mode amplitude grows because more ions become trapped near the resonance in the phase-space island. This study is in agreement with the result of Fig. 9. The observed correlation of the flux ratio with q(0) is caused by the correlation of the crash driven redistribution with q(0), which serves as an initial condition to further convective transport driven by chirping frequency magnetic fluctuation.

SUMMARY

In this paper we have developed a model for internal redistribution of fast trapped ions due to a large amplitude m = 2/n = 1 infernal kink mode instability at the q = 2 location. The model qualitatively describes the NPA measurements of redistribution of ICRF driven trapped hydrogen minority ions in JET ITB plasmas. Most importantly, the model predicts that the trajectories of ion bounce points after the instability become increasingly vertical when the core safety factor q(0) just before the instability increases above unity. This is consistent with the NPA measurements in which the magnitude of vertical displacement of ions is correlated with the value of q(0) before the instability. This agreement allows the conclusion that distinctive features particle redistribution accosiated with the kink like insta-bility as well as Kadomtsev reconnection in case of reconnection give the observed result. Magnetic field stochasticity, invoked in modeling of α-particle redistribution due to sawteeth in TFTR, can be excluded. In JET ITB plasma experiments, additional ion transport was observed when the instability was followed by a magnetic island with chirping frequency. Modeling of convective transport of resonant ions trapped in a radially moving phase-space island describes the main features of the observations.

ACKNOWLEDGEMENTS

The authors are grateful to to B. Alper and R. Budny for data analysis in support of this work, and to T. Hender, P. Helander and Yu. Yakovenko for valuable comments. This work was performed in part under the U.S. Department of Energy contract DE-AC02-76CH03073 and in part under the European Fusion ment Agreement. UKAEA authors were funded jointly by the UK Department of Trade and Industry, and by Euratom.

REFERENCES

[1]. M.P.Petrov, R.Bell, R.V.Budny, N.N.Gorelenkov, S.S.Meadley, R.B.White, and S.J.Zweben, Physics of Plasmas **6** 2430 (1999).

[2]. O. N. Jarvis, J. M. Adams, P. J. A. Howarth, F. B. Marcus, G. J. Sadler, E. Righi, D. F. H. Start, P. van Belle, C. D. Warrick, and N. Watkins, Nucl. Fusion, **36** 1513 (1996).

[3]. N.N.Gorelenkov, R.V.Budny, H.H.Duong, R.K.Fisher, S.S.Medley, M.P.Petrov, and M.H.Redi, Nuclear Fusion **37** 1053 (1997).

[4]. Ya.I.Kolesnichenko, V.V.Lutsenko, Yu.V.Yakovenko, and G.Kamelander, Physics of Plasmas **4** 2544 (1997).
[5]. Yi Zhao and R.B.White, Physics of Plasmas **4** 1103 (1997).
[6]. C.Gormezano and The JET Team, in Fusion Energy 1996 (Proc. 16th Int. Conf. Montreal, 1996), IAEA, Vienna, **1** 487 (1997).
[7]. G.T.A.Huysmans, T.C.Hender, B.Alper, et.al., Nuclear Fusion **30** 1489 (1999).
[8]. L.E.Zakharov, Nuclear Fusion, **18** 335 (1978).
[9]. A.I.Kislyakov, A.V.Khudoleev, S.S.Kozlovskij and M.P.Petrov, Fusion Engineering and Design, **34-35** 107 (1997).
[10]. A.A.Korotkov and A.Gondhalekar, 21st EPS Conference on Controlled Fusion and Plasma Physics, Europhysics Conference Abstracts, **18B**, Part I, 266 (1994).
[11]. A.A Korotkov, A.Gondhalekar, and A.J.Stuart, Nuclear Fusion, **37** 35 (1997).
[12]. K.G.McClements, R.O.Dendy and A.Gondhalekar, Nuclear Fusion, **37** 473 (1997).
[13]. V.I.Afanasiev, Y.Kusama, M.Nemoto, et.al., Plasma Physica and Controlled Fusion **39** 1509 (1997).
[14]. D.F.H.Start, J.Jacquinot, V.Bergeaud, et al., Physical Review Letters **80** 4681 (1998).
[15]. L-G.Eriksson, M.Mantsinen, D.Borba, et al., Physical Review Letters **81** 1231 (1998).
[16]. A.A.Korotkov, A.Gondhalekar and R.J.Akers, Proceedings of 5th IAEA TCM on Energetic Particles in Magnetic Confinement Systems, Culham, UK, 1997.
[17]. A.A.Korotkov, A.Gondhalekar and R.J.Akers, JET Report JET-P(98)25.
[18]. A.A.Korotkov, A.Gondhalekar and R.J.Akers, Physics of Plasmas **7** 957 (2000).
[19]. A.Gondhalekar, N.N.Gorelenkov, A.A.Korotkov, S.E.Sharapov and D.Testa, Proceedings of 6th IAEA TCM on Energetic Particles in Magnetic Confinement Systems, JAERI, Japan, October 1999, **and** Proceedings of 7th IAEA TCM on Energetic Particles in Magnetic Confinement Systems, Göteborg, Sweden, October 2001.
[20]. S.Bernabei, M.G.Bell, R.Budny, D.Darrow, E.D.Fredrickson, N.N.Gorelenkov, J.Hosea,et.al., Physics of Plasmas, **6** 1880 (1999), **and** Physical Review Letters, **84** 1212 (2000).
[21]. R.B.White, M.S.Chance, Physics of Fluids **27** 2455 (1984).
[22]. P.Helander, C.G.Gimblett, R.J.Hastie, et al., Physics of Plasmas, **4** 2181 (1997).
[23]. Z.Chang, W.Park, E.D.Fredrikson, et al., Physical Review Letters, **77** 3553 (1996).
[24]. C.T.Hsu, C.Z.Cheng, P.Helander, et al., Physical Review Letters, 72 2503 (1994).
[25]. C.Z.Cheng and M.S.Chance, Journal of Computational Physics 71 124 (1987).
[26]. R.V.Budny, Nuclear Fusion **32** 429 (1992).
[27]. C.T.Hsu, D.J.Sigmar, Physics of Fluids **B4** 1492 (1992).

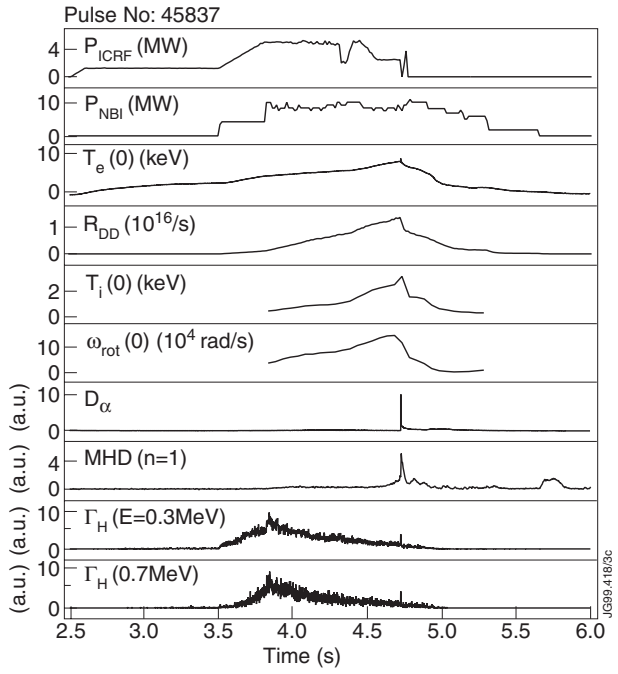

Figure 1: Evolution of pertinent parameters in a ITB plasma Pulse No: 45837 with $B_{\varphi 0}$ = 2.53T, I_{φ} = 2:32MA, q(0) = 1.65. Evolution is shown of the ICRF and NBI heating powers, peak electron temperature $T_e(0)$, DD fusion rate R_{DD}, peak ion temperature $T_i(0)$, central toroidal rotation frequency $\omega_{rot}(0)$, edge emission of D_α, and amplitude of n = 1mode. $\overline{\Gamma}_H$, the flux of hydrogen atoms to the NPA, is shown for two different energies $\mathcal{E}_H$, 0.3MeV and 0.7MeV.

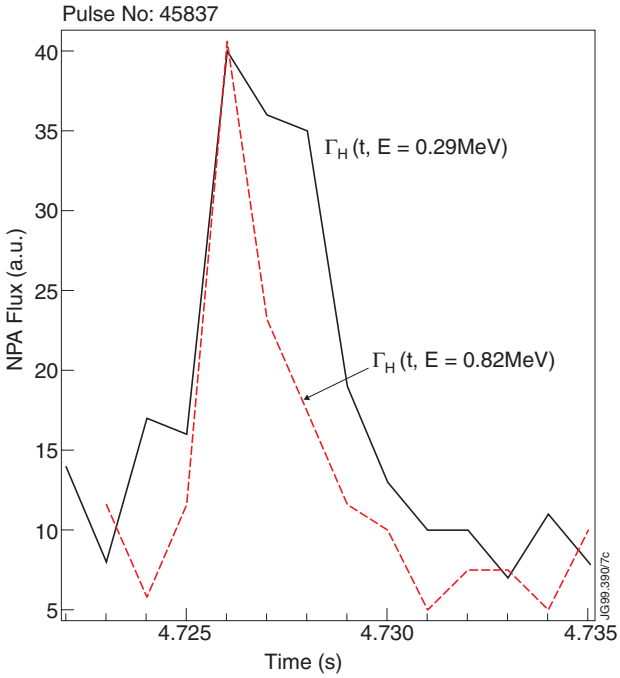

Figure 2: Evolution of NPA flux-spike at two representative energies, in a pulse with a long-lived magnetic island with chirping frequency following the n = 1 burst, showing energy dependent decay time of the flux-spike. We infer that larger the ion energy, faster is the decay of density of those ions.

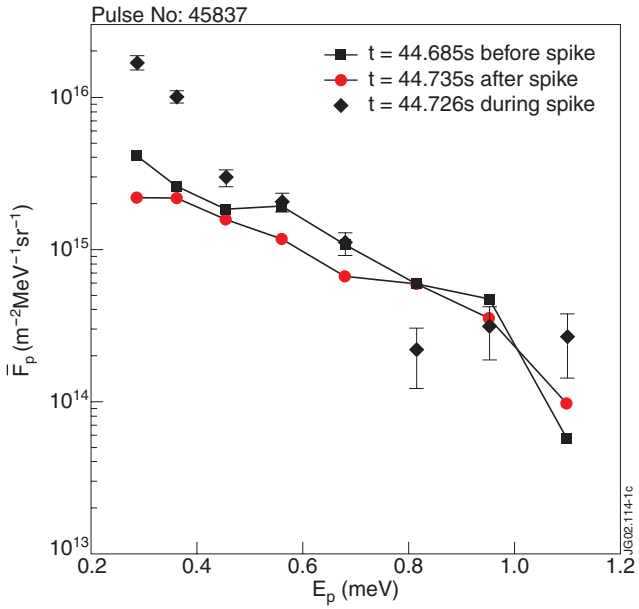

Figure 3: Measured energy distribution function of ions before, during and after the flux-spike averaged over 5msec time window. We see that the magnitude of $\overline{F}(\mathcal{E})$ after the flux-spike is reduced from that before the spike. We also see that more low energy ions are displaced than higher energy ones.

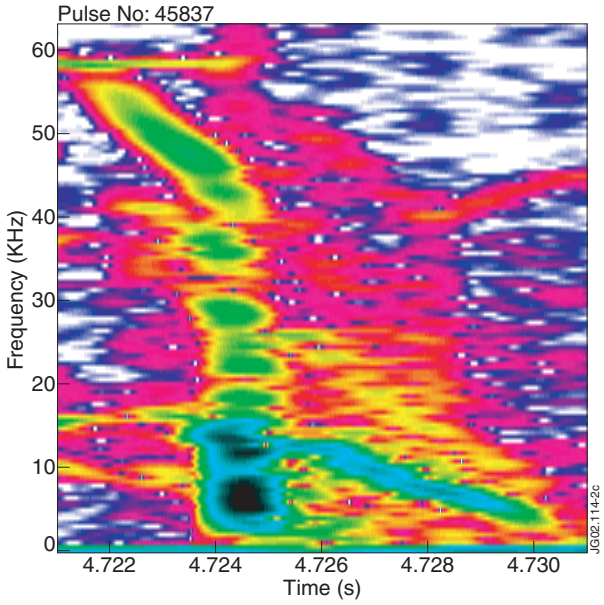

Figure 4: Spectrogram of B_θ fluctuations, showing the magnetic field activity at the time of the crash, and the subsequent long-lived n = 1magnetic field fluctuation, which had the form of the magnetic island with characteristic chirping frequency. During the crash typically $\delta B_\theta/B_s \geq 3\times10^{-4}$, whereas the frequency chirping magnetic island has $\delta B_\theta/B_s \approx 2\times10^{-4}$.

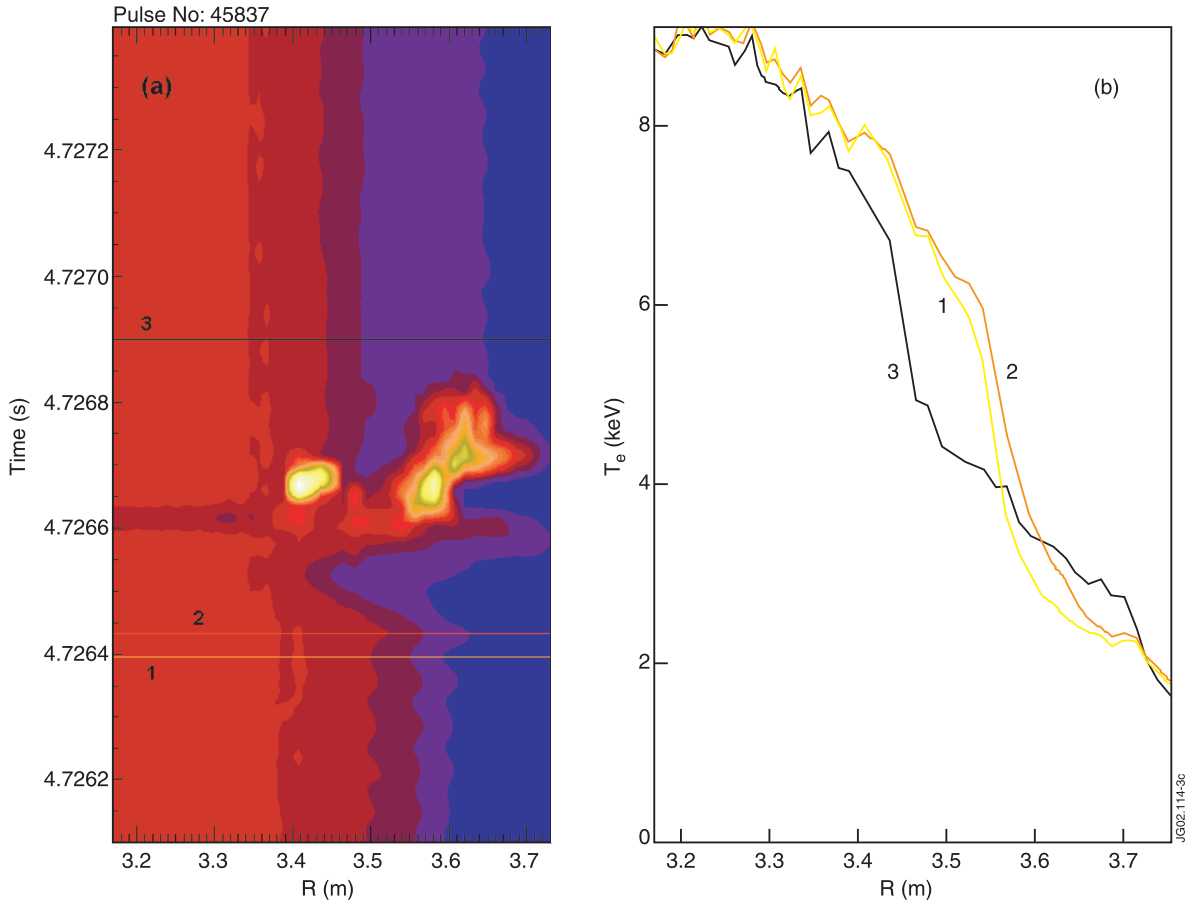

Figure 5: ECE measurement showing: (a) Contours of constant T_e as function of major radius R(m) and time t(s). At the crash cold plasma invades the region of higher T_e, followed by a period of intense non-thermal ECE emission. (b) Snapshot of T_e profile at three time points shown in fig.5(a), profiles #1 and #2 are at opposite phases of the precursor oscillation before the crash, illustrating the kink-like structure of the mode. Profile #3 is taken after the crash and shows the characteristic flattening inside the magnetic island, which persists for the ≈5ms duration of the frequency chirping shown in fig.4.

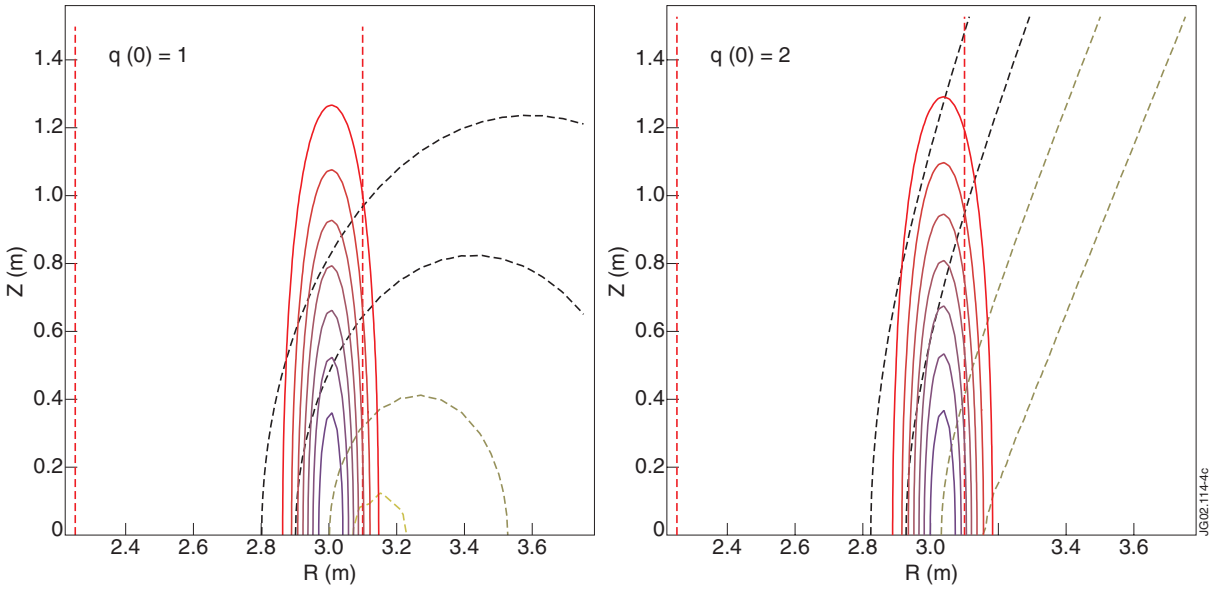

Figure 6: Contours of initial spatial distribution of energetic trapped ions, and characteristic trajectories of ion bounce point motion during the crash. Shown also is the vertical NPA line-of-sight. Bounce point trajectories are shown for the two limiting cases of (a) q(0) = 1, and (b) q(0) = 2. We have taken R_c = 3m, R_0 = 3.1m, and Δ_R = 0.1m, close to the experimental set-up.

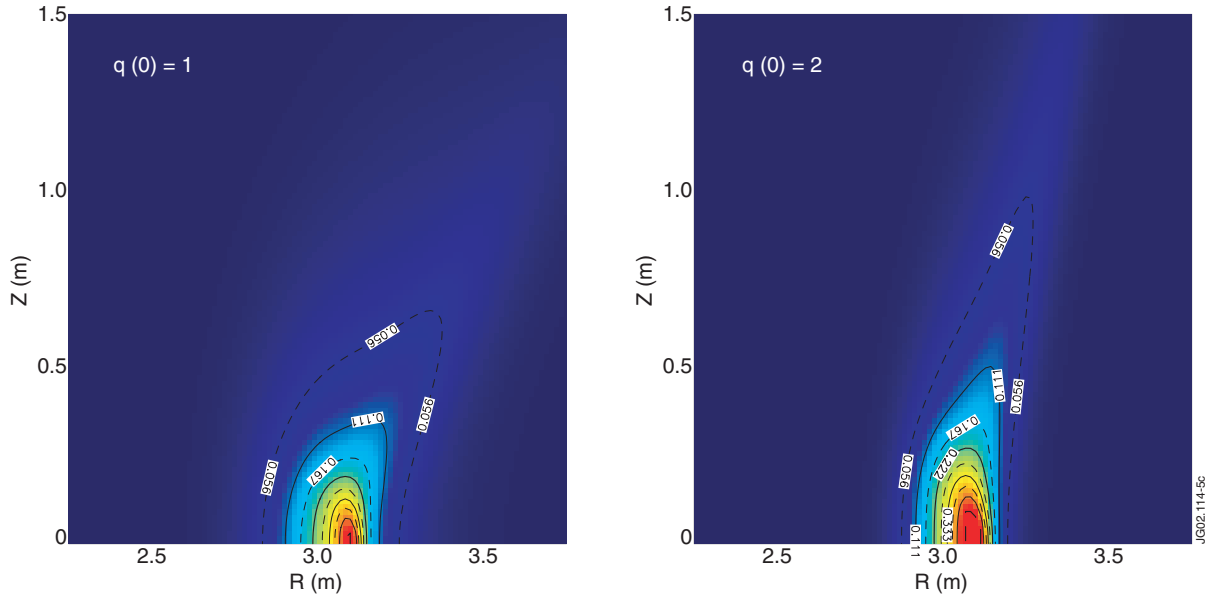

Figure 7: Spatial distribution of energetic trapped hydrogen ions after the kink instability, for cases with q(0) = 1 (left) and q(0) = 2(right), and for the initial distribution given by the Eq.(9).

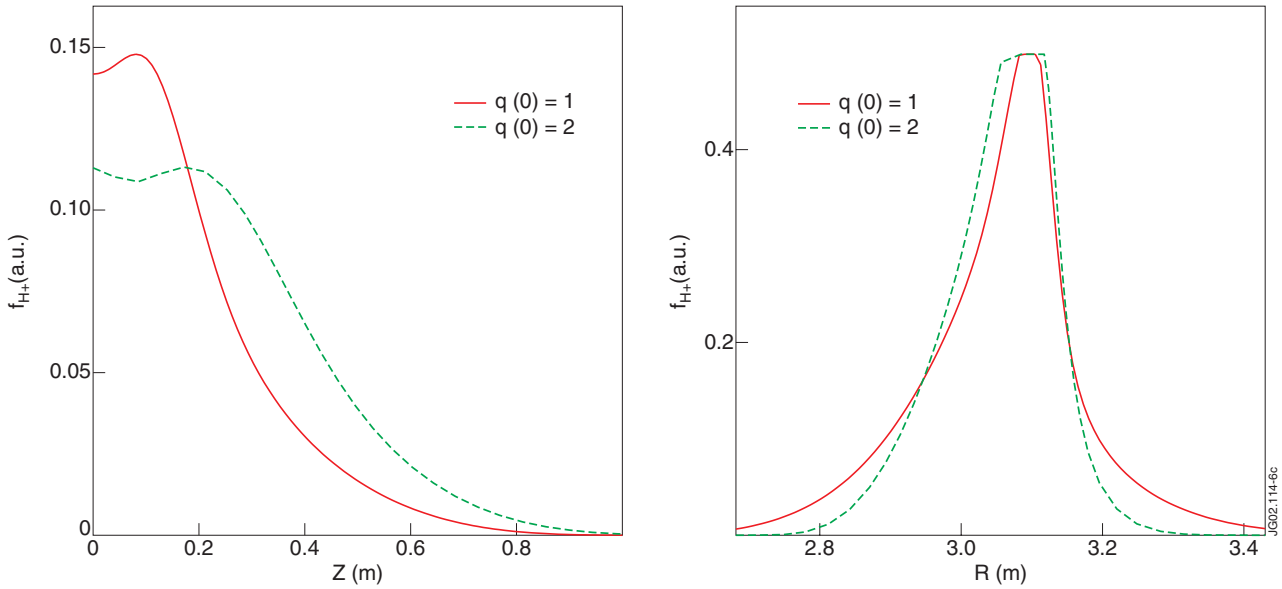

Figure 8: Energetic trapped hydrogen ion distribution after the instability, for twolimiting cases of q(0) = 1 and q(0) = 2, showing that the redistribution of ion bounce points along the vertical (left) and major-radius(right) axis is strongly dependent on the value of q(0).

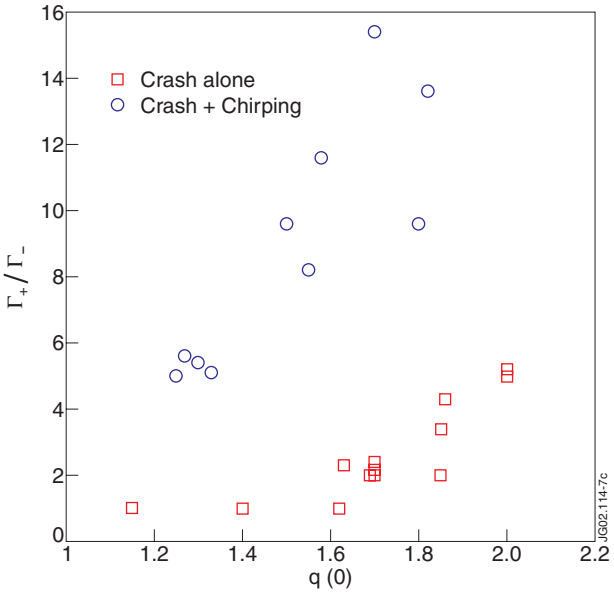

Figure 9: Ratio of flux to the NPA at the flux-spike (after the crash) to that just before it, as function of core safety factor q(0) for pulses with the crash alone and pulses with the crash and subsequent chirping frequency magnetic activity. q(0) here was determined using EFIT employing only external magnetic measurements.

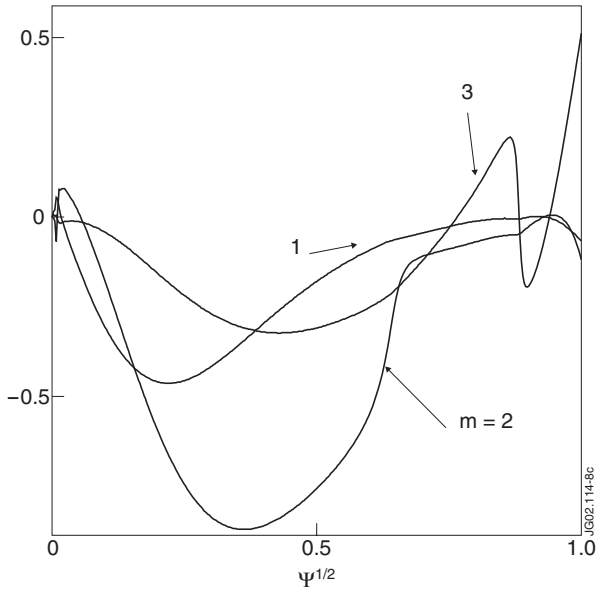

Figure 10: Dominant poloidal harmonics of the component of plasma displacement ξ perpendicular to the equilibrium magnetic flux surfaces, for the n = 1kink mode, calculated using ideal MHD stability code NOVA, for Pulse No: 45837 just before the crash. $\xi \cdot \nabla \Psi$ as function of $\sqrt{\Psi}$ is shown.

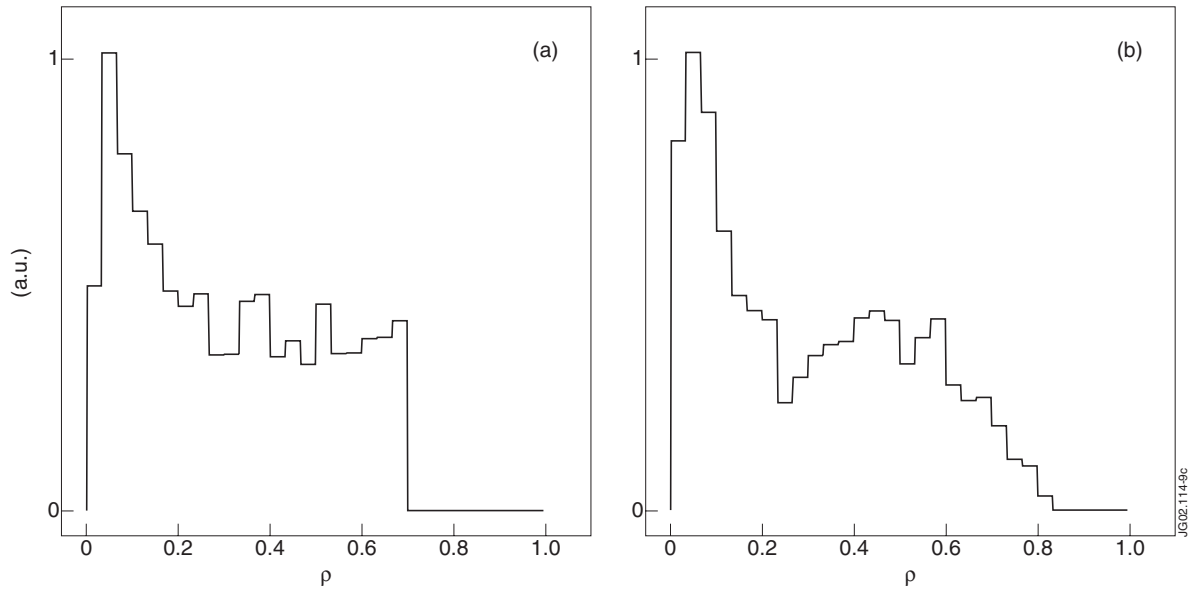

Figure 11: Minor radius distribution of energetic ion density, (a) initial flat spatial density distribution as input to computation, and (b) radial ion transport due to resonant interaction with chirping frequency magnetic fluctuations.

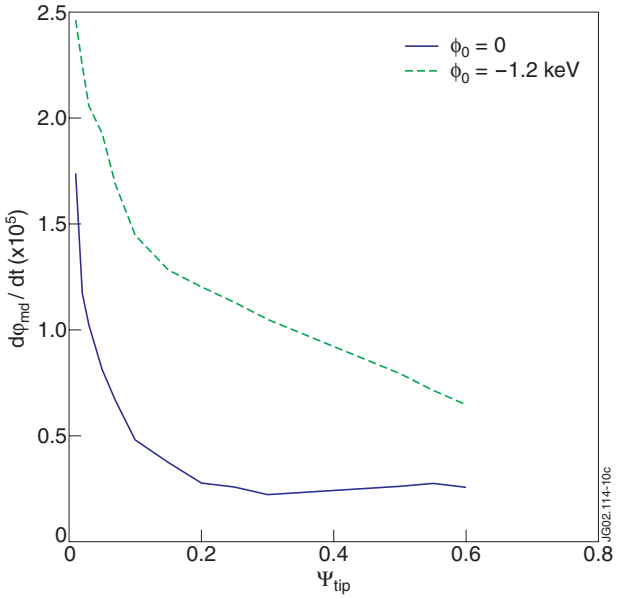

Figure 12: Toroidal precession frequency of a 200keV ion as a function of normalized poloidal flux at the bounce point of ion banana orbit with and without radial electric field.

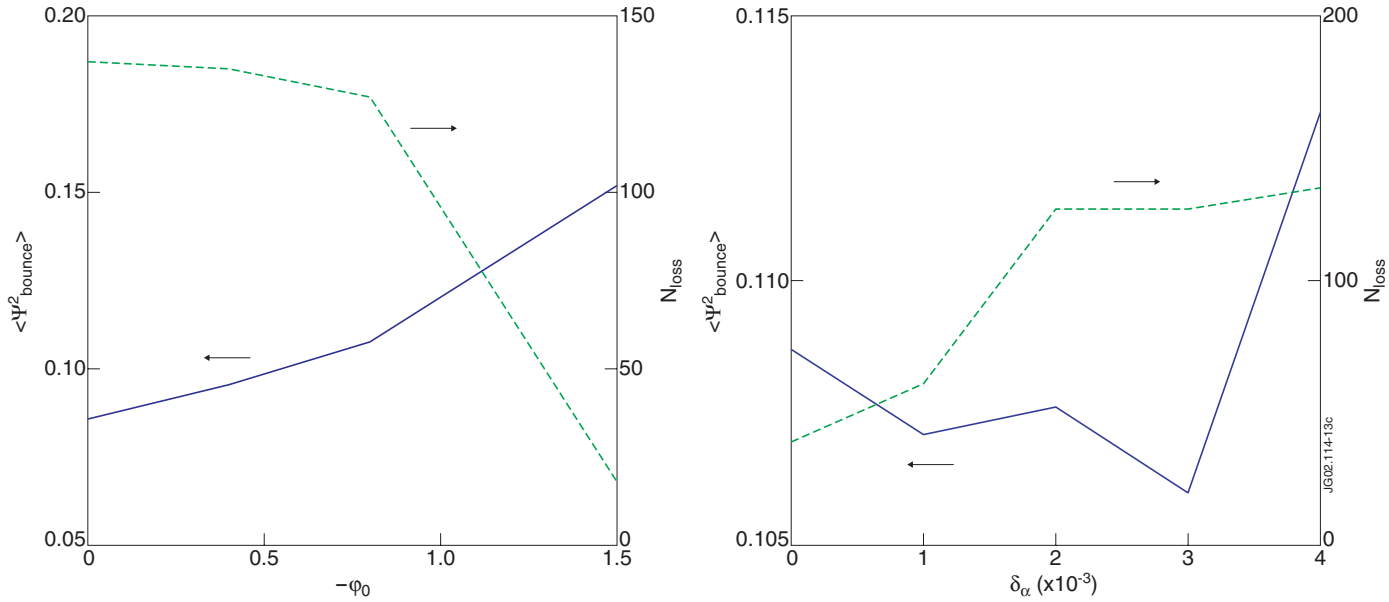

Figure 13: Characteristics of convective ion transport. Shown are the dependences of $<\Psi^2_{bounce}>$, squared poloidal flux at the ion bounce point averaged over the ion distribution, and a number of lost ions N_{loss} as functions of electric field potential ϕ_0 and $\delta\alpha$.